ϕ meson propagation in a hot hadronic gas

L. Alvarez-Ruso and V. Koch
Nuclear Science Division,
Lawrence Berkeley National Laboratory
1 Cyclotron Rd., Berkeley, CA 94720, USA

The Hidden Local Symmetry Lagrangian is used to study the interactions of ϕ mesons with other pseudoscalar and vector mesons in a hadronic gas at finite temperature. We have found a significantly small ϕ mean free path (less than 2.4 fm at $T > 170$ MeV) due to large collision rates with ρ mesons, kaons and predominantly K^* in spite of their heavy mass. This implies that ϕ mesons produced after hadronization in relativistic heavy ion collisions will not leave the hadronic system without scattering. The effect of these interactions on the time evolution of the ϕ density in the expanding hadronic fireball is investigated.

PACS numbers: 25.75.-q, 14.40.Ev, 24.10.Pa, 12.39.Fe

I. INTRODUCTION

Enhanced strangeness production in relativistic nucleus-nucleus collisions compared to nucleon-nucleon collisions has been predicted to be a consequence of the formation of quark-gluon plasma (QGP) [1]. This effect leads to an enhancement in the number of strange and multistrange particles produced after hadronization. In particular, free $s\bar{s}$ pairs would coalesce to form ϕ mesons, while their production in pp and πp collisions should be OZI suppressed [2]. On the other side, the ϕ mass is expected to decrease due to both many body effects in the hadronic medium [3, 4] and chiral symmetry restoration, which might generate a double peak structure [5]. The decay width is also modified (broadened) through the scattering with other particles [6–8].

The ϕ is a nice probe since it is not masked behind other resonances in the mass spectra. It decays, among several other possibilities, into kaon pairs (K^+K^-), and more rarely into dileptons (e^+e^-, $\mu^+\mu^-$); both channels have been detected at CERN-SPS [9–11]. Dileptons have negligible final state interactions with the hadronic environment, so they sense the entire evolution of the system. On the contrary, detectable kaons from ϕ decay probably emerge only at freezeout.

It is widely accepted that the ϕ mean free path (MFP) in the hot hadronic fireball is large due to the small cross section for scattering with nonstrange hadrons. This implies that ϕ spectra would retain the information about the stage of the collision at which the plasma hadronizes [2]. Available calculations [6–8] seem to support this idea. For example, in Ref. [7] the ϕ MFP was calculated taking into account its scattering with different mesons. Phenomenological Lagrangians with couplings extracted from the experimental partial decay rates were used. The obtained MFP at $T = 200$ MeV is rather big ($\lambda = 4.4$ fm) compared to the standard size of the hadronic system. Adding the reactions with nucleons and nucleonic resonances did not change qualitatively the situation [8].

However, ϕ production in $Pb - Pb$ collisions at SPS shows some intriguing features that are difficult to match with the picture of a ϕ weakly interacting with the hadronic medium. Both absolute yields and inverse slope parameters in the transverse mass (m_t) distributions exhibit different values when measured via $\mu^+\mu^-$ or K^+K^- decays [12]. The inverse slope, as obtained from the hadronic measurement, suggests that the ϕ's flow together with pions, kaons and protons, while the dilepton measurement is consistent with the assumption of an early freezeout. It has also been observed that the rapidity distribution (extracted from kaon pairs) in $Pb - Pb$ is about 50 % broader than in pp [9]. The origin could be attributed to longitudinal flow [13]. The modification of visible ϕ spectra due to kaon rescattering inside the fireball is an important ingredient but does not fully explain the discrepancies. Indeed, Johnson et al. [14] show that kaon rescattering can account for the observed rapidity distributions, but not for the differences in the m_t spectra, neither the inverse slopes, nor the relative yields.

Here we calculate ϕ collision rates and mean free path in a hot hadronic gas of pseudoscalar (π, K) and vector mesons (ρ, ω, K^*, ϕ). The reaction cross sections are obtained within the Hidden Local Symmetry Lagrangian (HSL) [15], which includes both Goldstone bosons and vector mesons in a manner consistent with the symmetries of QCD. The use of such a realistic model allows us to take into account many mechanisms that are not present in calculations that rely only in couplings extracted from observed decays but are allowed by the symmetries. This is, for instance, the case of vertices like ϕK^*K, ρK^*K^* and many others. As a consequence, we shall see that at temperatures between 150 and 200 MeV the ϕ mean free path in hadronic matter is considerably smaller than what has been estimated so far. Finally, we study the implications of these findings for the ϕ yields.

II. THE HIDDEN LOCAL SYMMETRY LAGRANGIAN

The HLS model provides a natural framework for describing the interactions between pseudoscalar and vec-

tor mesons. It is based on the fact that a $[\mathrm{U(3)_L}\times \mathrm{U(3)_R}]/\mathrm{U(3)_V}$ non-linear sigma model is gauge equivalent to another one with $[\mathrm{U(3)_L}\times\ \mathrm{U(3)_R}]_{\mathrm{global}}\times[\mathrm{U(3)_V}]_{\mathrm{local}}$ symmetry. The most general Lagrangian possessing this symmetry and made with the smallest number of derivatives is [16]

$$\mathcal{L} = \mathcal{L}_A + a\mathcal{L}_V\,, \tag{1}$$

$$\mathcal{L}_A = -\frac{1}{4}f_\pi^2\left\langle\left(D_\mu\xi_L\cdot\xi_L^\dagger - D_\mu\xi_R\cdot\xi_R^\dagger\right)^2\right\rangle\,, \tag{2}$$

$$\mathcal{L}_V = -\frac{1}{4}f_\pi^2\left\langle\left(D_\mu\xi_L\cdot\xi_L^\dagger + D_\mu\xi_R\cdot\xi_R^\dagger\right)^2\right\rangle\,, \tag{3}$$

where f_π stands for the pion decay constant and a is an arbitrary parameter; it is usually set to $a=2$, which allows to recover the standard vector meson dominance expression (VMD) [16, 17], although a slightly bigger value has been extracted from experiment [18]. The symbol $\langle\rangle$ denotes flavor trace. The covariant derivatives of the fields $\xi_{L,R}$ are

$$D_\mu\xi_{L(R)} = \left(\partial_\mu - igV_\mu\right)\xi_{L(R)}\,, \tag{4}$$

with V_μ being the dynamical gauge bosons of the hidden local symmetry, further identified with the nonet of vector mesons

$$V_\mu \equiv V_\mu^a T^a$$
$$= \frac{1}{\sqrt{2}}\begin{pmatrix} \frac{1}{\sqrt{2}}\rho_\mu^0 + \frac{1}{\sqrt{2}}\omega_\mu & \rho_\mu^+ & K_\mu^{*+} \\ \rho_\mu^- & -\frac{1}{\sqrt{2}}\rho_\mu^0 + \frac{1}{\sqrt{2}}\omega_\mu & K_\mu^{*0} \\ K_\mu^{*-} & \bar{K}_\mu^{*0} & \phi_\mu \end{pmatrix}. \tag{5}$$

Working in the unitary gauge i.e. choosing $\xi_{L,R}$ such that

$$\xi_L^\dagger = \xi_R = \xi = \exp i\Phi/f_\pi \tag{6}$$

$\mathcal{L}_\mathrm{A}$ becomes identical to the lowest order chiral Lagrangian

$$\mathcal{L}_\mathrm{A} = \frac{f_\pi^2}{4}\langle\partial_\mu U\partial_\mu U^\dagger\rangle\,, \tag{7}$$

with $U=\xi^2$; Φ is the octet of pseudoscalar Goldstone bosons

$$\Phi = \frac{1}{\sqrt{2}}\begin{pmatrix} \frac{1}{\sqrt{2}}\pi^0 + \frac{1}{\sqrt{6}}\eta & \pi^+ & K^+ \\ \pi^- & -\frac{1}{\sqrt{2}}\pi^0 + \frac{1}{\sqrt{6}}\eta & K^0 \\ K^- & \bar{K}^0 & -\frac{2}{\sqrt{6}}\eta \end{pmatrix}. \tag{8}$$

The physics contained in $\mathcal{L}_V$ becomes clear when ξ is expanded up to the term linear in Φ

$$\xi \approx 1 + i\frac{\Phi}{f_\pi}\,. \tag{9}$$

Then,

$$\mathcal{L}_V = \frac{1}{2}ag^2f_\pi^2V_\mu^aV^{\mu a} - i\frac{a}{2}g\langle\{[\Phi,\partial_\mu\Phi]\,,V^\mu\}\rangle\,, \tag{10}$$

where $[,]$ and $\{,\}$ stand for commutator and anticommutator respectively. Vector mesons have acquired mass $m_V^2 = ag^2f_\pi^2$ by spontaneous breakdown of the hidden local symmetry. One now assumes that a kinetic term for them is generated by the underlying QCD dynamics or quantum effects at the composite level [16, 17]. Thus, we have

$$\mathcal{L}_{kin} = -\frac{1}{2}\langle F_{\mu\nu}F^{\mu\nu}\rangle\,, \tag{11}$$

$F_{\mu\nu}$ being the nonabelian field strength tensor

$$F_{\mu\nu} = \partial_\mu V_\nu - \partial_\nu V_\mu - ig\left[V_\mu, V_\nu\right]\,. \tag{12}$$

Substituting Eq. (12) into (11) we obtain, apart from the standard kinetic terms, the interactions of 3 and 4 vector mesons

$$\mathcal{L}_{VVV} = ig\langle\left(\partial_\mu V_\nu - \partial_\nu V_\mu\right)[V^\mu, V^\nu]\rangle \tag{13}$$

$$\mathcal{L}_{VVVV} = -\frac{g^2}{2}\langle[V_\mu, V_\nu]\,[V^\mu, V^\nu]\rangle \tag{14}$$

As we shall see, these terms generate large contributions to the total cross section of the ϕ meson with other hadrons, specially vector mesons.

In order to account for deviation from the flavor symmetry one should add $[\mathrm{U(3)_L}\times\ \mathrm{U(3)_R}]_{\mathrm{global}}$ breaking terms which do not affect the hidden symmetry. There is no unique way to do this. Different implementations are studied in Ref. [19]. Here we adopt the scheme proposed in Ref. [20], in which $\mathcal{L}_A$ and $\mathcal{L}_V$ are modified as follows

$$\mathcal{L}_A + \Delta\mathcal{L}_A = -\frac{1}{4}f_\pi^2\left\langle\left(D_\mu\xi_L\cdot\xi_L^\dagger - D_\mu\xi_R\cdot\xi_R^\dagger\right)^2\ \times \right.$$
$$\left.\left(1 + \xi_L\epsilon_A\xi_R^\dagger + \xi_R\epsilon_A\xi_L^\dagger\right)\right\rangle\,, \tag{15}$$

$$\mathcal{L}_V + \Delta\mathcal{L}_V = -\frac{1}{4}f_\pi^2\left\langle\left(D_\mu\xi_L\cdot\xi_L^\dagger + D_\mu\xi_R\cdot\xi_R^\dagger\right)^2\ \times \right.$$
$$\left.\left(1 + \xi_L\epsilon_V\xi_R^\dagger + \xi_R\epsilon_V\xi_L^\dagger\right)\right\rangle\,, \tag{16}$$

with $\epsilon_{A(V)} = \mathrm{diag}(0,0,c_{A(V)})$; $c_{A(V)}$ are real parameters to be determined. After fixing the gauge (Eq. 6) and expanding ξ (Eq. 9), one observes that the kinetic terms in

$\mathcal{L}_A$ have to be renormalized. This is achieved by rescaling [20]

$$\sqrt{1+c_A}\,K \to K\,, \quad \sqrt{1+\frac{2}{3}c_A}\,\eta \to \eta\,. \tag{17}$$

Such a redefinition leads to the following relations for the pseudoscalar meson decay constants

$$f_K = \sqrt{1+c_A}\,f_\pi\,, \quad f_\eta = \sqrt{1+\frac{2}{3}c_A}\,f_\pi\,. \tag{18}$$

Now, different vector mesons have different masses

$$m_\rho^2 = m_\omega^2 = \frac{m_{K^*}^2}{1+c_V} = \frac{m_\phi^2}{1+2c_V} = a f_\pi^2 g^2\,, \tag{19}$$

while the second term in Eq. (10), which describes the coupling of vector mesons to a pair of pseudoscalar ones, looks like

$$\mathcal{L}_{VPP} = -i\frac{a}{2}g\langle\{[\Phi,\partial_\mu\Phi]\,,V^\mu\}\,(1+2\epsilon_V)\rangle\,. \tag{20}$$

Eq. (16) contains also a vector-vector-pseudoscalar-pseudoscalar contact term

$$\mathcal{L}_{VVPP} = -ag^2\left\langle V_\mu V^\mu\left(\epsilon_V\Phi^2+2\Phi\epsilon_V\Phi+\Phi^2\epsilon_V\right)\right\rangle\,. \tag{21}$$

Obviously, the flavor symmetry is also broken in the pseudoscalar sector. The corresponding Lagrangian can be written as

$$\mathcal{L}_{SB} = \frac{1}{4}f_\pi^2\left\langle\xi_L\chi\xi_R^\dagger+\xi_R\chi\xi_L^\dagger\right\rangle\,, \tag{22}$$

where χ can be expressed in terms of π and K masses

$$\chi = \mathrm{diag}(m_\pi^2, m_\pi^2, 2m_K^2-m_\pi^2) \tag{23}$$

assuming the same mass for both u and d quarks.

It is known that the local chiral symmetry is broken at the quantum level. The anomalous part of the Lagrangian in terms of effective degrees of freedom is obtained assuming that the anomaly at composite level should coincide with that at constituent level. In the framework of HLS, vector mesons were incorporated to the anomalous Lagrangian by Fujikawa et al. [21]. It contains the vector-vector-pseudoscalar interaction. In Ref. [22], the flavor breaking effect was included by introducing a term $(\xi_L\epsilon_{WZ}\xi_R^\dagger+\xi_R\epsilon_{WZ}\xi_L^\dagger)$, with $\epsilon_{WZ} = \mathrm{diag}(0,0,c_{WZ})$, so that the total anomalous Lagrangian reads

$$\begin{aligned}&\mathcal{L}_{VVP}+\Delta\mathcal{L}_{VVP}\\ &= 2g_{VVP}\epsilon^{\mu\nu\lambda\sigma}\left\langle\partial_\mu V_\nu\,(1+2\epsilon_{WZ})\,\partial_\lambda V_\sigma\,\Phi\right\rangle\,.\end{aligned} \tag{24}$$

The coupling constant is fixed by the anomaly

$$g_{VVP} = \frac{3g^2}{8\pi^2 f_P}\,, \quad P=(\pi,K,\eta)\,, \tag{25}$$

and c_{WZ} is directly obtained from the ratio between the experimental decay widths of $K^{*0}\to K^0\gamma$ and $K^{*\pm}\to K^\pm\gamma$ [22].

III. COLLISION RATES AND MEAN FREE PATH

A. General formulae

The propagation of ϕ mesons through the hot hadronic gas depends on how often they interact in their way out of the fireball. For a given binary reaction $1+2\to 3+4$, the number of collisions per unit time at a given temperature is described by the average collision rate

$$\Gamma_{coll}(T) = \frac{d_1 d_2}{n_1}\int\prod_{i=1}^4\frac{d^3p_i}{2E_i(2\pi)^3}\overline{|\mathcal{M}|^2}\times$$

$$(2\pi)^4\delta^{(4)}(p_1+p_2-p_3-p_4)f_1f_2(1+f_3)(1+f_4) \tag{26}$$

where $\overline{|\mathcal{M}|^2}$ stands for the amplitude squared, summed over final spins and averaged over initial ones; d_i are the spin degeneracy factors $d_i = 2S_i+1$ (we take care of the isospin degeneracy by considering each isospin channel independently), while f_i represent the momentum distributions. The particle number density is given by

$$n_1 = d_1\int\frac{d^3p_1}{(2\pi)^3}f_1 \tag{27}$$

Approximating all momentum distributions by Boltzmann

$$f_i \approx e^{-E_i/T}\,, \quad 1+f_i\approx 1+e^{-E_i/T}\approx 1\,, \tag{28}$$

and, identifying the particle labeled 1 with the ϕ meson, one gets

$$\begin{aligned}\Gamma_{coll}^{(2)}(T) &= \frac{d_2}{4\pi^2 m_\phi^2 K_2(m_\phi/T)}\times\\ &\int_{(m_\phi+m_2)^2}^\infty ds\sqrt{s}p_{cm}^2\sigma(s)K_1(\sqrt{s}/T)\end{aligned} \tag{29}$$

with s and p_{cm} being the center-of-mass (CM) energy squared and three-momentum respectively and $\sigma(s)$, the total cross section; index (2) denotes the particle that collides with the ϕ.

The most straightforward way to estimate the relevance of rescatterings in the medium is to compute the mean free path and compare it with the size of the system. For the mean free path we use

$$\lambda(T) = \frac{\bar v}{\Gamma_{coll}^t}\,; \tag{30}$$

$\bar v$ is the average velocity of the ϕ in the medium

$$\bar v = \frac{d_1}{n_1}\int\frac{d^3p_1}{(2\pi)^3}f_1\frac{|\mathbf{p}_1|}{E_1} = \frac{2T(T+m_\phi)}{m_\phi^2 K_2(m_\phi/T)}e^{-m_\phi/T}\,; \tag{31}$$

the expression on the right is obtained assuming a Boltzmann distribution. $\Gamma_{coll}^t = \sum_a\Gamma_{coll}^{(a)}$ arises from the contribution of all relevant hadronic reactions. In the present calculation we have $a=\pi,K,\rho,\omega,K^*,\phi$.

B. Binary Reactions

Within the HLS model described in Section II one can compute all possible binary reactions of ϕ mesons with $\pi, K, \rho, \omega, K^*, \phi$ at tree level. The interaction vertices are given by the VPP, VVP, VVV VVVV and VVPP Lagrangians defined in Eqs. (20, 24, 13, 14, 21) respectively. There are three classes of Feynman diagrams, which are depicted in Fig. 1 and represent s-channel (s), t-channel (t) and contact (c) reaction mechanisms. The reactions

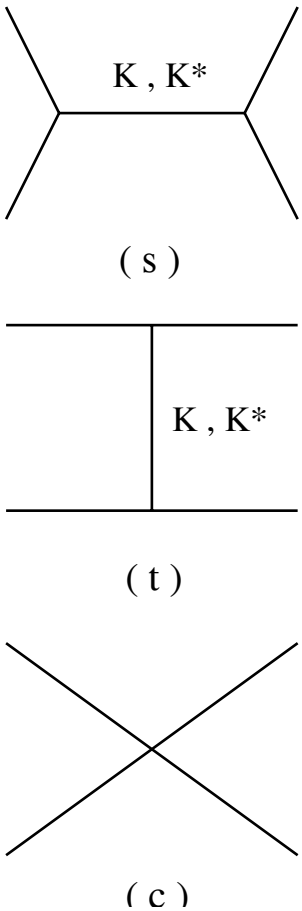

FIG. 1: Generic Feynman diagrams for the different reaction mechanisms; (s) stands for s-channel, (t) for t-channel and (c) for contact.

considered in the present study are listed in Table I. The OZI rule manifests itself in the absence of direct couplings of ϕ's with π, ρ or ω mesons in the model. Therefore, only s and t diagrams with a strange particle (K or K^*) in the intermediate state appear. This is also the reason why s-channel mechanisms are only present in the case of ϕ collisions with strange mesons. Notice that there are two kinds of contact terms: the VVPP vertex, which appears as a result of symmetry breaking and the VVVV vertex obtained from the kinetic part of the Lagrangian.

Explicit expressions of the Lagrangian for the different vertices are written in Appendix A. They are derived

No.	Reaction	Channels
1.1	$\phi + \pi \to K + K$	t(K^*)
1.2	$\phi + \pi \to K + K^*$	t(K, K^*), c
1.3	$\phi + \pi \to K^* + K^*$	t(K, K^*)
2.1	$\phi + K \to \pi + K$	s,t(K^*)
2.2	$\phi + K \to \rho + K$	s,t(K, K^*)
2.3	$\phi + K \to \omega + K$	s,t(K, K^*)
2.4	$\phi + K \to \phi + K$	s,t(K, K^*), c
2.5	$\phi + K \to \pi + K^*$	s(K, K^*), t(K^*)
2.6	$\phi + K \to \rho + K^*$	s,t(K, K^*)
2.7	$\phi + K \to \omega + K^*$	s,t(K, K^*)
2.8	$\phi + K \to \phi + K^*$	s,t(K, K^*)
3.1	$\phi + \rho \to K + K$	t(K, K^*)
3.2	$\phi + \rho \to K + K^*$	t(K, K^*)
3.3	$\phi + \rho \to K^* + K^*$	t(K, K^*), c
4.1	$\phi + \omega \to K + K$	t(K, K^*)
4.2	$\phi + \omega \to K + K^*$	t(K, K^*), c
4.3	$\phi + \omega \to K^* + K^*$	t(K, K^*), c
5.1	$\phi + K^* \to \pi + K$	s(K^*), t(K, K^*), c
5.2	$\phi + K^* \to \rho + K$	s,t(K, K^*)
5.3	$\phi + K^* \to \omega + K$	s,t(K, K^*)
5.4	$\phi + K^* \to \phi + K$	s,t(K, K^*)
5.5	$\phi + K^* \to \pi + K^*$	s,t(K, K^*)
5.6	$\phi + K^* \to \rho + K^*$	s,t(K, K^*), c
5.7	$\phi + K^* \to \omega + K^*$	s,t(K, K^*), c
5.8	$\phi + K^* \to \phi + K^*$	s,t(K, K^*), c
6.1	$\phi + \phi \to K + K$	t(K, K^*), c
6.2	$\phi + \phi \to K + K^*$	t(K, K^*), c
6.3	$\phi + \phi \to K^* + K^*$	t(K, K^*), c

TABLE I: List of binary reactions of ϕ's with pseudoscalar (π, K) and vector (ρ, ω, K^*, ϕ) mesons. s, t and c correspond to the diagrams in Fig. 1 while the particles in brackets denote the intermediate mesons.

by substituting the matrices of Eqs. (5,8) in the generic Lagrangians of Eqs. (20, 24, 13, 14, 21), taking the trace and rescaling the kaon field as shown in Eq. (17). From those Lagrangians it is straightforward to compute the Feynman rules for the vertices. We use the standard expressions for the meson propagators

$$D_K(q) = \frac{i}{q^2 - m_K^2 + i\, m_K \Gamma_K^{(tot)}(q^2)}\,, \qquad (32)$$

$$D_{K^*}^{\mu\nu}(q) = -\left(g^{\mu\nu} - \frac{q^\mu q^\nu}{m_{K^*}^2}\right) \times \frac{i}{q^2 - m_{K^*}^2 + i\, m_{K^*} \Gamma_{K^*}^{(tot)}(q^2)}\,. \qquad (33)$$

$\Gamma_{K(K^*)}^{(tot)}$ stand for the total decay widths of the intermediate K, K^* and include all decay channels that are open

for a given q^2 value. Using the Lagrangians introduced above one gets

$$\Gamma_K^{(tot)} = \sum_{a=\rho,\omega,\phi} \left\{ \Gamma_{K\to a\,K}(q^2)\,\theta\left(q^2-(m_a+m_K)^2\right) + \Gamma_{K\to a\,K^*}(q^2)\,\theta\left(q^2-(m_a+m_K^*)^2\right)\right\} \quad (34)$$

and

$$\Gamma_{K^*}^{(tot)} = \sum_{a=\pi,\rho,\omega,\phi} \left\{ \Gamma_{K^*\to a\,K}(q^2)\,\theta\left(q^2-(m_a+m_K)^2\right) + \Gamma_{K^*\to a\,K^*}(q^2)\,\theta\left(q^2-(m_a+m_K^*)^2\right)\right\}, \quad (35)$$

where $\theta(x)$ is the standard step function. Explicit expressions for the different decay widths are listed in Appendix B. By introducing such imaginary parts in the propagators, we are implementing an approximate unitarization for the s-channel diagrams. Hence, we have included in the decay widths only those channels that are considered in the final state. The contribution to the width of one of the ignored channels $K \to K(\pi\pi)_{L=0}$ can be readily computed using Lagrangians (7, 22) and is found to be negligible.

Since hadrons are extended objects, it is necessary to insert form factors that suppress high momentum transfers. This affects all t-channel Feynman diagrams. We adopt the widely used monopole form

$$F_i(q^2) = \frac{\Lambda^2 - m_i^2}{\Lambda^2 - q^2}, \quad i = K,\, K^* \quad (36)$$

assuming the same cutoff parameter $\Lambda = 1.8$ GeV for all species [6, 7]. These form factors cause a strong reduction in the t-channel contributions to the collision rates.

The amplitude squared for the VVVV term is quite large and increases very fast with s since it involves high powers of both g and s (g^4 and s^4). As a consequence, higher order corrections become relevant as one goes away from threshold. We take approximately into account the resummation of s-channel loops in the contact amplitude for $\phi + a \to b + c$ by means of the substitution

$$\alpha g^2 \to \frac{\alpha g^2}{\left[1+\alpha g^2 G(s,m_\phi,m_a)\right]^{1/2}\left[1+\alpha g^2 G(s,m_b,m_c)\right]^{1/2}}, \quad (37)$$

with

$$G(s,m_a,m_b) = -i\frac{1}{2\pi}\frac{p_{cm}}{\sqrt{s}}\left[1+\frac{(s-m_a^2-m_b^2)^2}{8m_a^2m_b^2}\right], \quad (38)$$

where p_{cm} is the momentum of the vector mesons a and b in the CM frame. The factor $\alpha = -1/2$ for the $\phi\phi K^*K^*$ vertex and $\alpha = 1/(2\sqrt{2})$ for $\phi\rho K^*K^*$ and $\phi\omega K^*K^*$. This ansatz is inspired by the solution of the Bethe-Salpeter (BS) equation in the K-matrix approximation using only the part of the tree-level amplitude, which leads to an algebraic equation (see Appendix C for details). $G(s,m_a,m_b)$ vanishes at threshold, so that one recovers the tree-level amplitude, and becomes progressively larger with the increase of s, causing an effective suppression of the coupling constant g. At large s, our simple expression shall become inaccurate compared with the solution of the full BS equation with couple-channels effects incorporated, but one should bare in mind that high values of s are exponentially suppressed in the integral that defines the collision rates in Eq. (29). Therefore, this inaccuracy has a small numerical impact in the determination of the collision rates, but is important to avoid artificially large contributions from cross section values above the unitarity limit.

With these ingredients, one can compute the amplitudes; it is important to add them coherently since the interferences modify appreciably the total cross section. A caveat is in order regarding reactions 1.2 and 2.4. In both cases the exchanged kaon (in the t-channel) can be put on the mass shell, making the amplitude become singular. The singularity disappears if one takes into account that kaons will develop an in-medium width [6, 7]. However, studying how the modifications of propagators, vertices or masses and widths of the particles involved in the reactions influence the collision rates goes beyond the scopes of the present work. Hence, we just do not take them into consideration. In any case, their contribution will most likely shorten the mean free path even more. The same is true for mechanisms that include baryons or heavier mesons, both in asymptotic and intermediate states (some of them have been studied in Refs. [7, 8]), as well as multiparticle production like $\phi + K(K^*) \to K + \pi + \pi$.

C. Results

The parameters of the HLS model can be fixed using the experimental values of masses and pseudoscalar decay constants. We choose a=2 after VMD; then, using the ρ mass in Eq. (19) and $f_\pi = 92.4$ MeV [23] one gets $g = 5.89$. Once a and g are fixed, the remaining part of Eq. (19) gives c_V. It ranges from 0.34 to 0.38 depending on weather determined from m_{K^*} or m_ϕ. We adopt $c_V = 0.36$. Next, from Eq. (18) and using the experimental value $f_K/f_\pi = 1.22$ [24], we obtain $c_A = 0.49$. Finally, we take $c_{WZ} = -0.1$ as determined in Ref. [22]. Isospin degeneracy is assumed, i.e. the mass differences between mesons of the same species are not taken into account.

The contributions of the different mesons to the ϕ collision rate as a function of temperature are shown in Fig. 2. For temperatures between 150 and 200 MeV, the collision rate is dominated by the K^* followed by K and ρ, while the contributions from π, ω and ϕ are smaller.

In order to understand why $\Gamma_{coll}^{(K^*)}$ is bigger than $\Gamma_{coll}^{(K)}$ in spite of their mass difference let us recall that $\Gamma_{coll}^{(a)}$ can

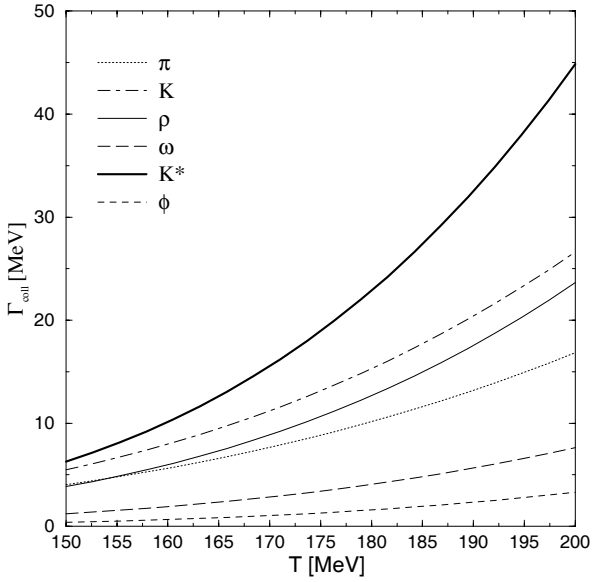

FIG. 2: Collision rates of ϕ with π, K, ρ, ω, K^* and ϕ as a function of temperature.

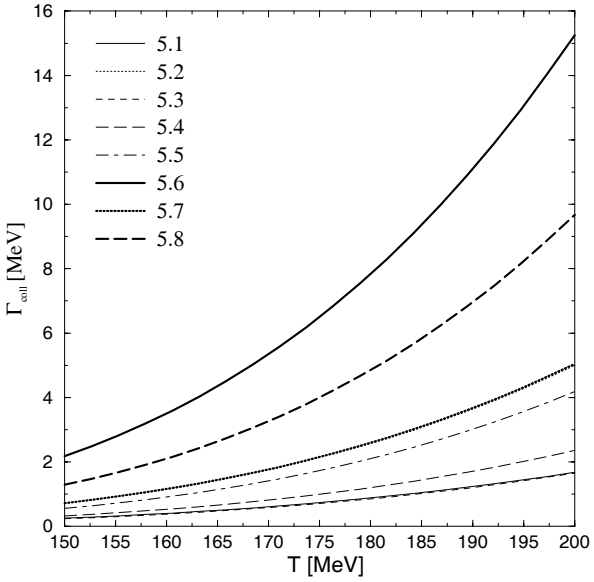

FIG. 3: Contribution from the various reactions of ϕ with K^* to the collision rates. The labels correspond to the reaction numbers in Table I. The largest rate is from $\phi + K^* \to \rho + K^*$. Notice that the contributions of reactions 5.1 and 5.3 as well as 5.2 and 5.7 almost coincide and are hardly distinguishable in the plots.

be cast as

$$\Gamma^{(a)}_{coll} = n_a \langle \sigma v_{rel} \rangle \,. \tag{39}$$

Hence, the averaged rate factor $\langle \sigma v_{rel} \rangle$ must overcome a ratio of (see Eq. 27)

$$\frac{n_{K^*}}{n_K} = \frac{3 m^2_{K^*} K_2(m_{K^*}/T)}{m^2_K K_2(m_K/T)} \,; \tag{40}$$

at $T = 200$ MeV this ratio is equal to 0.77. This number is much bigger than what one would naively expect. In fact, the small number coming from the ratio of Bessel functions is almost compensated by the ratio of squared masses times the spin degeneracy. The former being due to the higher density of states for a heavy particle. Therefore, a larger $\Gamma^{(K^*)}_{coll}$ can be achieved by a *moderately* larger cross section. The comparison between Figs. 3 and 4 show that the reactions involving all four vector mesons make the true difference between $\Gamma^{(K^*)}_{coll}$ and $\Gamma^{(K)}_{coll}$, and the mechanisms involving VVVV and VVV vertices given in Eqs. (13, 14) are responsible for this.

The sum of all partial rates of Fig. 2 is shown in Fig. 5. It is considerably bigger than what has been predicted in all previous works [6–8]. In this case, the major novel ingredient is the dynamics involving different vector mesons as shown above. The dashed line represents the contribution of all ϕ-number changing reactions; that is, all reactions in Table I except the (quasi)elastic ones 2.4, 2.8, 5.4 and 5.8. The inelastic reactions account for more than 80 % of the total collision rate.

We have also studied the sensitivity of the result to the modification of parameters in the HLS model. It was found to depend appreciably on the value of g, which is

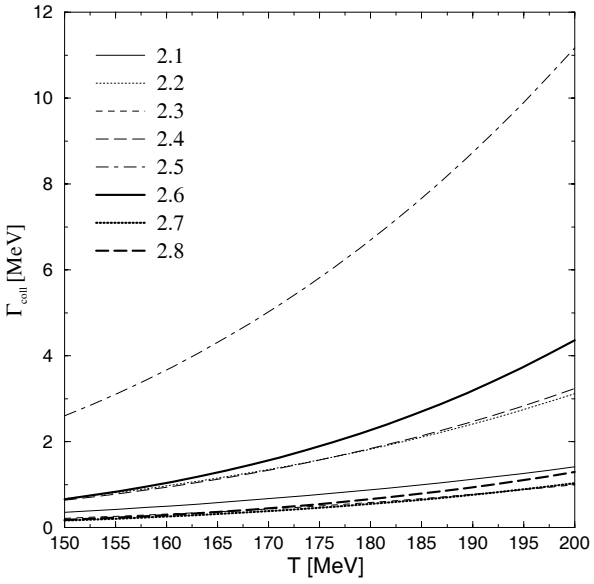

FIG. 4: Contribution to the collision rate of ϕ with K from the different reactions listed in Table I.

not surprising since the cross sections involve high powers of this coupling (up to g^8). As mentioned in Section II, the value of a extracted from the experiment is slightly bigger than 2. If we take $a = 2.4$ [18], then a lower limit of $g = 5.38$ is obtained. We fix the upper limit by using m_ω instead of m_ρ, getting $g = 5.98$. The region of

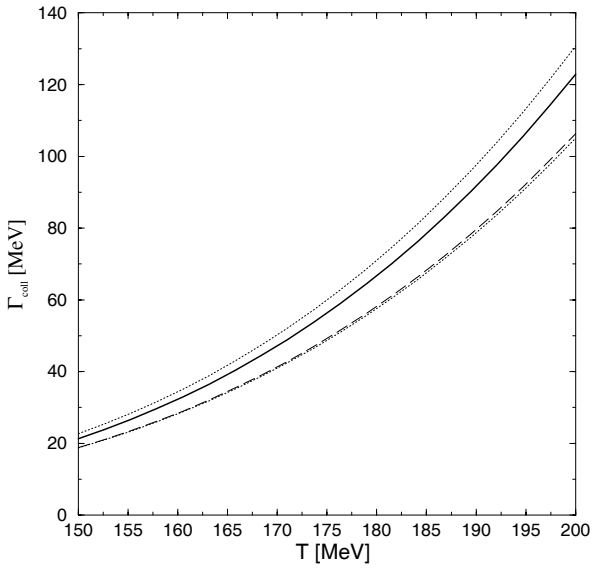

FIG. 5: Total collision rate of ϕ meson as a function of temperature (solid line). The dotted lines constrain the region of possible values when the model parameters are changed as described in the text. The dashed line is the contribution from ϕ-number changing processes alone.

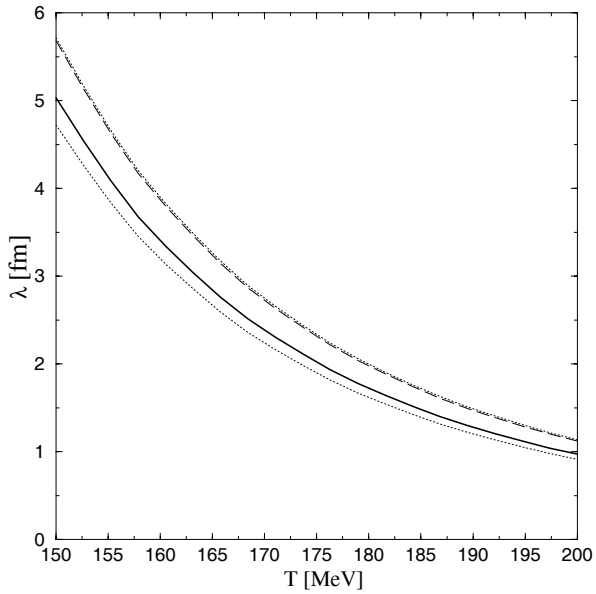

FIG. 6: Temperature dependence of the ϕ mean free path in hot hadronic matter. Line styles have the same meaning as in Fig. 5.

possible values of Γ_{coll} is bounded by the dotted lines in Fig. 5.

In Fig. 6 we show the ϕ mean free path as a function of temperature. It goes below 2.4 fm at $T > 170$ MeV. This is much smaller than the typical size of the hadronic system created in heavy ion collisions (10-15 fm). Therefore, contrary to the common believe [2], the ϕ mesons that are created after hadronization, at temperatures presumably between 170 and 200 MeV, will not leave the fireball without interacting; they will most likely be absorbed and reemitted in the hadronic phase. The uncertainties discussed above do not modify this conclusion.

IV. TIME EVOLUTION

We now proceed to study qualitatively the time evolution of the ϕ density in the expanding hadronic fireball. It is governed by the following rate equation

$$\partial_\mu \left(n_\phi u^\mu \right) = \Psi \tag{41}$$

where $u^\mu = \gamma(1, \boldsymbol{\nu})$ is the four velocity, defined in terms of the Lorentz factor γ and the fluid velocity $\boldsymbol{\nu}$; Ψ stands for the source term

$$\Psi = - \sum_{a,b,c} \langle \sigma_{\phi a \to bc} v_{\phi a} \rangle n_\phi n_a + \sum_{a,b,c} \langle \sigma_{bc \to \phi a} v_{bc} \rangle n_b n_c - \sum_{b,c} \langle \Gamma_{\phi \to bc} \rangle n_\phi + \sum_{b,c} \langle \sigma_{bc \to \phi} v_{bc} \rangle n_b n_c \,, \tag{42}$$

which takes into account ϕ-number changing processes: binary collisions, decay, recombination. In this approach, the evolution of momentum distribution is not investigated. Kinetic equilibrium (and the applicability of the hydrodynamical description) is assumed, but not chemical equilibrium [25, 26].

In principle, Eq. (41) is just one in a system of coupled equations that describes the time evolution of the densities of all species. Such a treatment would require the knowledge of the reaction cross sections for all the mesons of the model. We shall rather perform the simplifying assumption that, at hadronization temperature, all particles (π, K, ρ, ω, K^*, ϕ) are in chemical equilibrium, and all of them except the ϕ remain in it until freezeout. In chemical equilibrium, detailed balance holds, i.e.

$$\langle \sigma_{\phi a \to bc} v_{\phi a} \rangle n_\phi^{eq} n_a^{eq} = \langle \sigma_{bc \to \phi a} v_{bc} \rangle n_b^{eq} n_c^{eq} \tag{43}$$

and

$$\langle \Gamma_{\phi \to bc} \rangle n_\phi^{eq} = \langle \sigma_{bc \to \phi} v_{bc} \rangle n_b^{eq} n_c^{eq} \,. \tag{44}$$

Substituting these equations in Eq. (42) and imposing that particle number densities for all species except ϕ's take their equilibrium values:

$$n_{a,b,c} = n_{a,b,c}^{eq} \,, \tag{45}$$

one obtains

$$\partial_\mu \left(n_\phi u^\mu \right) = -\Gamma \left(n_\phi - n_\phi^{eq} \right) \,, \tag{46}$$

where $n_\phi^{eq}(T)$ comes directly from Eqs. (27, 28)

$$n_\phi^{eq}(T) = \frac{3}{2\pi^2} m_\phi^2 T K_2 \left(\frac{m_\phi}{T} \right) \,; \tag{47}$$

$\Gamma(T)$ denotes the number of interactions per unit time and is split in two parts

$$\Gamma(T) = \Gamma_{coll}(T) + \Gamma_{dec}(T)\,. \tag{48}$$

Γ_{coll} is the collision rate calculated in the previous Section. Notice however that the right hand side of Eq. (46) does not hold for collisions of two ϕ mesons $\phi + \phi \to b + c$ (reactions 6.1-6.3). The reason being that ϕ's are not in chemical equilibrium. For our simple estimate we thus ignore those processes which are very small (see short-dashed line in Fig 2). Analogously, the contribution of (quasi)elastic reactions $\phi + a \to \phi + c$ (2.4, 2.8, 5.4, 5.8) to the source term Ψ vanishes if particles a and c are in chemical equilibrium. As we have already stated, these reactions account for less than 20 % of the total collision rate in Fig 5.

$\Gamma_{dec}(T)$ is the average free decay width. For the sake of consistency we only consider decays into kaon pairs, which account for 83 % of the total width. The general expression for Γ_{dec} is a trivial modification of Eq. (26). Proceeding as in Section III A one gets

$$\Gamma_{dec}(T) = \Gamma_0 \frac{K_1(m_\phi/T)}{K_2(m_\phi/T)}\,, \tag{49}$$

where $\Gamma_0 = 3.7$ MeV. Obviously, at high temperatures, Γ_{dec} is negligible compared to Γ_{coll}, but the later drops fast when the system cools down.

In central relativistic heavy ion collisions the distribution of matter is approximately uniform in rapidity, at least in the central rapidity region, and the geometry of the collision is cylindrically symmetric [27]. Therefore, it is convenient to adopt as coordinates $\{\tau, \eta, r, \varphi\}$ where r and φ are the transverse radius and polar angle, while τ and η represent the *longitudinal* proper time and space-time rapidity respectively

$$\tau = \sqrt{t^2 - z^2}\,, \quad \eta = \frac{1}{2}\ln\frac{t+z}{t-z}\,. \tag{50}$$

The assumptions of a radial transverse expansion and Lorentz invariance in the central region imply that $u^\eta = u^\varphi = 0$. Next, assuming a uniform density distribution in the transverse plane and averaging over the radial coordinate (analogously to what was done in Refs. [25, 26] for the spherically symmetric case) we get

$$\frac{1}{\tau R^2(\tau)}\frac{\partial}{\partial\tau}\left\{\tau R^2(\tau) n_\phi \langle u^\tau\rangle\right\} = -\Gamma(T)\left(n_\phi - n_\phi^{eq}\right)\,, \tag{51}$$

which is to be solved with the initial condition $n_\phi(\tau_0) = n_\phi^{eq}(T_0)$, τ_0 and T_0 being the hadronization time and temperature; $R(\tau)$ is the transverse radius of the system. Notice that $\tau\pi R^2$ is nothing but the volume of the expanding fireball at mid-rapidity. The averaged τ component of the four velocity is given by

$$\langle u^\tau\rangle = \frac{2}{R^2(\tau)}\int_0^{R(\tau)} dr\, r u^\tau(r)\,. \tag{52}$$

Following Ref. [28], we assume that the flow vector u^μ can be constructed from two independent boosts, one in the longitudinal and another in the radial direction. Then, it is easy to see that at mid-rapidity

$$u^\tau = \gamma_r = \frac{1}{\sqrt{1-\beta_r^2}}\,. \tag{53}$$

A reasonable ansatz for radial velocity is [28]

$$\beta_r(\tau, r) = \beta_s\left(\frac{r}{R}\right)^a\,. \tag{54}$$

In the case of a constant β_s

$$\langle u^\tau\rangle = \int_0^1 dy\,\frac{1}{\sqrt{1-\beta_s^2 y^a}} \tag{55}$$

is a constant too. Using the boundary condition

$$\frac{dR}{d\tau} = \beta_r(\tau, R) = \beta_s \tag{56}$$

one gets

$$R(\tau) = \beta_s(\tau - \tau_0) + R_0\,, \tag{57}$$

where $R_0 = 1.2\,A^{1/3}$ fm is the radius of the colliding nuclei.

Finally, in order to solve the rate equation we need the relation between time and temperature, which can be derived from entropy conservation

$$\partial_\mu\,(s u^\mu) = 0\,. \tag{58}$$

Repeating the same procedure as for n_ϕ one finds

$$\frac{1}{\tau R^2(\tau)}\frac{\partial}{\partial\tau}\left\{\tau R^2(\tau) n_\phi \langle u^\tau\rangle\right\} = 0\,. \tag{59}$$

This equation can be easily solved, obtaining the following implicit expression for $\tau(T)$ (or vice versa)

$$\tau R^2(\tau)\langle u^\tau\rangle(\tau) s(T) = \tau_0 R_0^2 \langle u^\tau\rangle(\tau_0) s(T_0)\,. \tag{60}$$

If $\langle u^\tau\rangle$ does not depend on τ, as for the ansatz considered above, Eq. (60) reflects that the total entropy in the central region of the collision is conserved.

The functional dependence of the entropy upon the temperature depends on the properties of the system under consideration. We describe it as an ideal gas of π, K, ρ, ω and K^* obeying Boltzmann statistics

$$s(T) = \sum_i \frac{g_i}{2\pi^2} m_i^3 K_3\left(\frac{m_i}{T}\right)\,, \tag{61}$$

with $i = \{\pi, K, \rho, \omega, K^*\}$; g denotes the degeneracy (both spin and isospin). The underlying idea is that the equation of state of a gas of free hadrons and resonances should mimic the one of a dense hadron gas [29].

Fig. 7 shows the τ dependence of the ratio of the ϕ yield at mid-rapidity $N(\tau) = \tau\pi R^2(\tau) n_\phi(\tau)$ and the number

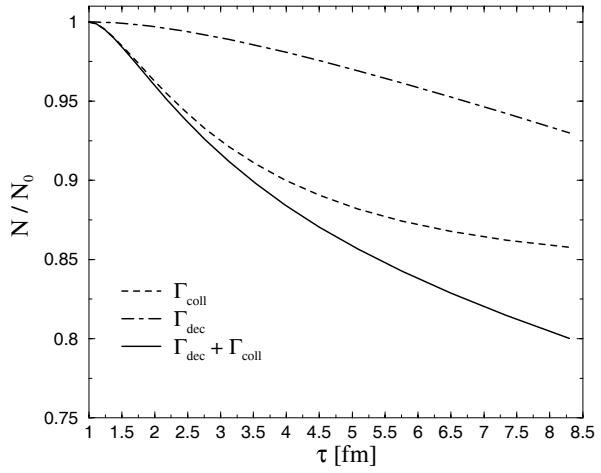

FIG. 7: Time dependence of the ratio of the ϕ number to its value at hadronization. The dashed line shows the contribution from inelastic collisions while the long-short dashed one accounts for free decay (and recombination) The combined effect of both collisions and free decay is described by the solid line.

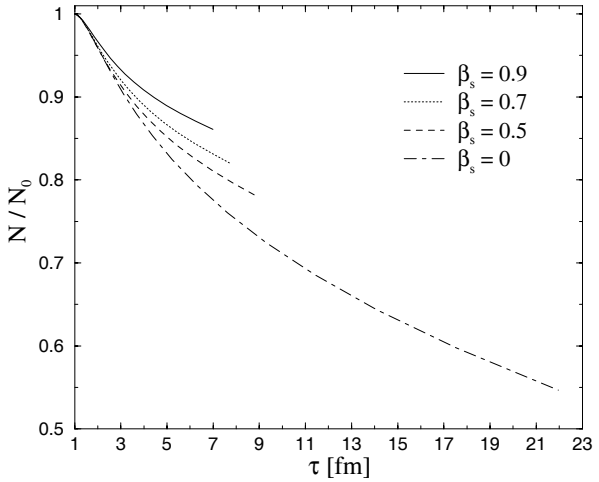

FIG. 8: Ratio of the ϕ number to its value at hadronization for different values of the transverse flow velocity at the surface. The end point of the lines correspond to a temperature of 100 MeV.

of them right after hadronization $N_0 = \tau_0 \pi R_0^2 n_\phi^{eq}(T_0)$. We have used $\tau_0 = 1$ fm, $T_0 = 190$ MeV, $\beta_s = 0.6$, $a = 1$ and $A = 197$ (Au).

At the early stages of the expansion, the system is hot and the collision rates are high, so that ϕ's are pushed towards equilibrium making its number decrease fast. As the system cools down, the collision rates become small and the contribution of the collision rates to the ratio starts to saturate. The effect of the decay is negligible below $\tau = 2$ fm, not only because $\Gamma_{dec} \ll \Gamma_{coll}$ but also because detailed balance works more efficiently than at lower temperatures. We have taken a freezeout temperature of $T_f = 100$ MeV, which corresponds to a life time of $\tau_f = 8.3$ fm. If one assumes that only those ϕ mesons present at freezeout are detectable via kaon pairs, then the ϕ yield is reduced in 20 % with respect to hadronization.

This model exhibits a notable dependence on the value of β_s, as illustrated in Fig 8. The bigger β_s, the faster the temperature drops and, hence, the closer N/N_0 gets to one. The case $\beta_s = 0$ corresponds to the Bjorken limit, where the transverse expansion is neglected. For our choice of the equation of state, this is a rather unrealistic situation because the system lives so long that the transverse expansion can not be neglected. For more realistic values of β_s we get a ratio N/N_0, at $T_f = 100$ MeV, between 0.78 and 0.86.

We have also considered different hadronization temperatures, as shown in Fig. 9. If the hadronization temperature is low, the collision rates are small from the very beginning, and the interactions become less relevant.

The present simple description of the time evolution of the ϕ number in an expanding hadronic gas is intended to illustrate the consequences of the short ϕ mean free path

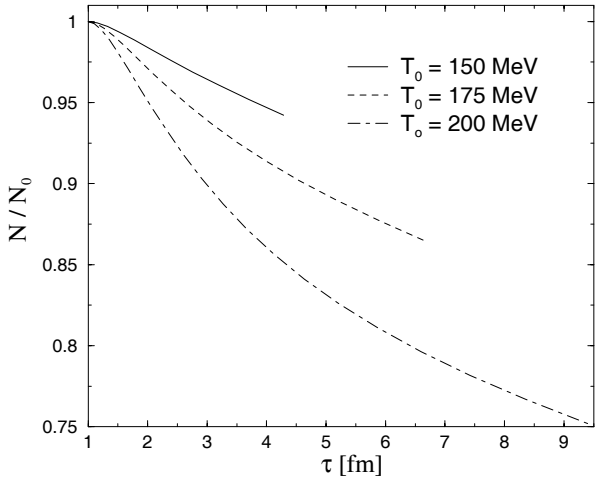

FIG. 9: Same as Fig. 8 but for different hadronization temperatures.

that we have obtained. A realistic analysis of the spectra would require a more sophisticated treatment. In particular, the fact that the ϕ collision rate is dominated by ϕ-number changing reactions implies that mainly those processes are responsible for maintaining the kinetic equilibrium via detailed balance. Therefore, if the system is out of chemical equilibrium, detailed balance no longer holds and the system will also depart from kinetic equilibrium. This means that both ϕ temperature and flow velocity will differ from those of other species with high rates of elastic scatterings like pions.

A. The role of chemical potentials

Up to now we have not introduced chemical potentials (fugacity factors) for any of the particle species under consideration. However, it is well known that when the number changing processes are not effective, particle numbers are fixed and chemical potentials associated with these conserved quantities appear [30, 31]. For pions and kaons values of $\mu_\pi = 60 - 80$ MeV and $\mu_K = 100 - 130$ MeV are reached at freezeout temperatures between 110 and 120 MeV [32].

In order to study the effect of such conserved meson numbers in the ϕ yield we assume that $\mu_i = 0$ at hadronization for all species and grows to a value μ_i^f at freezeout. A simple linear interpolation is used in between:

$$\mu_i(T) = \frac{T_0 - T}{T_0 - T_f}\mu_i^f \, . \tag{62}$$

We take $\mu_\pi^f = 70$ MeV, $\mu_K^f = 115$ MeV with $T_f = 115$ MeV to be consistent with the values quoted above. Since $\rho \leftrightarrow \pi\pi$ is a fast process, one can say that π and ρ mesons are in relative chemical equilibrium i.e. $\mu_\rho = 2\mu_\pi$ [31]. In the case of the ω, a recent calculation has obtained a large collision rate for the reaction $\omega\pi \to \pi\pi$ at high temperatures [33]; therefore, we take $\mu_\omega = \mu_\pi$. With the K^* the situation is uncertain because its decay width into $K\pi$ (51 MeV) might or might not be large enough to ensure a relative chemical equilibrium. Since the K^*'s are important for the ϕ yield due to their large contribution to the collision rate, we consider here two possibilities. The first is the assumption of chemical equilibrium via $K^* \leftrightarrow K\pi$, so that $\mu_{K^*} = \mu_K + \mu_\pi$ and the second is that the K^* has its own chemical potential, which we keep equal to the initial one $\mu_{K^*} = 0$ for the sake of simplicity.

The presence of chemical potentials implies that the condition (45) should be replaced by

$$n_{a,b,c} = n^\mu_{a,b,c} = n^{eq}_{a,b,c} e^{\frac{\mu_{a,b,c}(T)}{T}} \, , \tag{63}$$

leading to the following rate equation

$$\begin{aligned} \partial_\mu \left(n_\phi u^\mu\right) =& -\sum_{a,b,c} \Gamma_{\phi a \to bc} \left(n_\phi e^{\frac{\mu_a(T)}{T}} - n_\phi^{eq} e^{\frac{\mu_b(T)+\mu_c(T)}{T}} \right) \\ & -\Gamma_{dec} \left(n_\phi - n_\phi^{eq} e^{\frac{2\mu_K(T)}{T}} \right) \, . \end{aligned} \tag{64}$$

The equation of state should also be modified. Now, instead of Eq. (61), we have

$$\begin{aligned} s(T) \;=\; & \sum_i \frac{g_i}{2\pi^2} m_i^3 \left\{ K_3\left(\frac{m_i}{T}\right) \right. \\ & - \left. \left[\frac{\mu_i(T)}{m_i} - \frac{T}{m_i}\frac{d\mu_i(T)}{dT} \right] K_2\left(\frac{m_i}{T}\right) \right\} \, . \end{aligned} \tag{65}$$

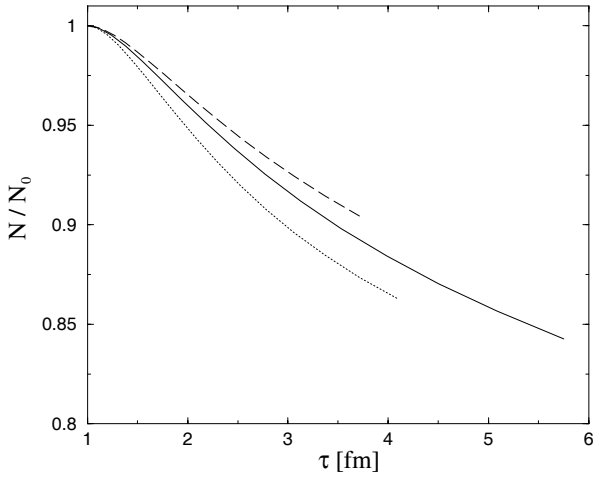

FIG. 10: Time dependence of the ratio N/N_0 at zero (solid line) and nonzero (dashed line) chemical potentials, as described in the text. The dotted line stands for the case of $\mu_{K^*} = 0$ while keeping $\mu_{\pi,K,\rho,\omega} \neq 0$.

The result for the ratio N/N_0 is given in Fig. 10. The solid line reproduces the calculation without chemical potentials. It corresponds to the solid line in Fig. 7 but ends earlier due to the higher freezeout temperature considered here. The introduction of chemical potentials causes an increase in the number of ϕ's as shown by the dashed line. In this case, the inverse reactions are favored keeping the ϕ number higher. The higher density at a given temperature also translates into a higher pressure and, therefore, a faster cooling and earlier freezeout. If one sets μ_{K^*} to zero while keeping the previous values for the other mesons (dotted line) then the tendency is inverted, and direct reactions are the most efficient. However, the final ϕ number is still bigger than in the $\mu_i = 0$ case due to the faster cooling of the hadron gas.

V. SUMMARY

We have studied ϕ interactions with a hot hadronic medium composed of π, K, ρ, ω, K^* and ϕ using the Hidden Local Symmetry model. In this way, we could take into account many vertices that are allowed by the symmetries of strong interactions but whose couplings cannot be directly determined experimentally. This is the case of three and four vector meson vertices which are responsible of the large collision rates of ϕ's with other vector mesons, specially K^*. As a consequence, we have shown that the ϕ mean free path at temperatures above 170 MeV is between 2.4 and 1 fm i.e. much smaller than the typical size of the hadronic system created in relativistic heavy ion collisions.

The implications of this result for the ϕ yield has been investigated by solving the rate equation for the ϕ density assuming kinetic but not chemical equilibrium. The

high collision rates at the early stages of the hadronic evolution tend to maintain the equilibrium, causing a reduction of the ϕ number with respect to hadronization. This decrease ranges from 5 % to 45 % depending on hadronization temperature, freezeout temperature and flow velocity. Finally, we have studied how the departure from chemical equilibrium of π, ρ, K and K^* mesons, taken into account the by introducing chemical potentials, influences the time evolution of the ϕ number.

Acknowledgments

We thank P. Huovinen and N. Xu for many helpful discussions. L.A.R. acknowledges a fellowship from the Spanish Ministry of Education and Culture. He also acknowledges the hospitality at the Theory Department, GSI, where part of this work was performed. This work was supported by the Director, Office of Science, Office of High Energy and Nuclear Physics, Division of Nuclear Physics, and by the Office of Basic Energy Sciences, Division of Nuclear Sciences, of the U.S. Department of Energy under Contract No. DE-AC03-76SF00098. L.A.R. has also been supported in part by Spanish DGICYT contract number BFM2000-1326.

APPENDIX A: FULL SET OF LAGRANGIANS

The explicit expressions of the Lagrangians describing the interaction vertices used in this work are listed below. A compact notation for π, K, ρ and K^* fields has been used; namely,

$$\pi \equiv \begin{pmatrix} \pi^0 & \sqrt{2}\pi^+ \\ \sqrt{2}\pi^- & -\pi^0 \end{pmatrix}, \qquad K \equiv \begin{pmatrix} K^+ \\ K^0 \end{pmatrix}, \qquad \bar{K} \equiv \begin{pmatrix} K^- & \bar{K}^0 \end{pmatrix}, \tag{A1}$$

and

$$\rho_\mu \equiv \begin{pmatrix} \rho_\mu^0 & \sqrt{2}\rho_\mu^+ \\ \sqrt{2}\rho_\mu^- & -\rho_\mu^0 \end{pmatrix}, \qquad K_\mu^* \equiv \begin{pmatrix} K_\mu^{*+} \\ K_\mu^{*0} \end{pmatrix}, \qquad \bar{K}_\mu^* \equiv \begin{pmatrix} K_\mu^{*-} & \bar{K}_\mu^{*0} \end{pmatrix}. \tag{A2}$$

From Eq. (20):

$$\mathcal{L}_{\rho KK} = i\frac{ag}{4}\frac{1}{1+c_{_A}}\left(\bar{K}\rho_\mu\partial^\mu K - \partial^\mu\bar{K}\rho_\mu K\right) \tag{A3}$$

$$\mathcal{L}_{\omega KK} = i\frac{ag}{4}\frac{1}{1+c_{_A}}\omega_\mu\left(\bar{K}\partial^\mu K - \partial^\mu\bar{K}K\right) \tag{A4}$$

$$\mathcal{L}_{\phi KK} = -i\frac{ag}{2\sqrt{2}}\frac{1+2c_{_V}}{1+c_{_A}}\phi_\mu\left(\bar{K}\partial^\mu K - \partial^\mu\bar{K}K\right) \tag{A5}$$

$$\mathcal{L}_{K^*K\pi} = i\frac{ag}{4}\frac{1+c_{_V}}{\sqrt{1+c_{_A}}}\left(\partial^\mu\bar{K}\pi K_\mu^* - \bar{K}_\mu^*\pi\partial^\mu K + \bar{K}_\mu^*\partial^\mu\pi K - \bar{K}\partial^\mu\pi K_\mu^*\right) \tag{A6}$$

From Eq. (24):

$$\mathcal{L}_{\rho K^*K} = \frac{g_{_{VVP}}}{2}\frac{1}{\sqrt{1+c_{_A}}}\epsilon^{\mu\nu\lambda\sigma}\left(\bar{K}\partial_\mu\rho_\nu\partial_\lambda K_\sigma^* + \partial_\lambda\bar{K}_\sigma^*\partial_\mu\rho_\nu K\right) \tag{A7}$$

$$\mathcal{L}_{\omega K^*K} = \frac{g_{_{VVP}}}{2}\frac{1}{\sqrt{1+c_{_A}}}\epsilon^{\mu\nu\lambda\sigma}\partial_\mu\omega_\nu\left(\bar{K}\partial_\lambda K_\sigma^* + \partial_\lambda\bar{K}_\sigma^*K\right) \tag{A8}$$

$$\mathcal{L}_{\phi K^*K} = \frac{g_{_{VVP}}}{\sqrt{2}}\frac{1+2c_{_{WZ}}}{\sqrt{1+c_{_A}}}\epsilon^{\mu\nu\lambda\sigma}\partial_\mu\phi_\nu\left(\bar{K}\partial_\lambda K_\sigma^* + \partial_\lambda\bar{K}_\sigma^*K\right) \tag{A9}$$

$$\mathcal{L}_{K^*K^*\pi} = \frac{g_{_{VVP}}}{2}(1+2c_{_{WZ}})\epsilon^{\mu\nu\lambda\sigma}\partial_\mu\bar{K}_\nu^*\pi\partial_\lambda K_\sigma^* \tag{A10}$$

From Eq. (13):

$$\mathcal{L}_{\rho K^* K^*} = i\frac{g}{2}\left\{\left(\partial_\mu \bar{K}^*_\nu - \partial_\nu \bar{K}^*_\mu\right)\rho^\mu K^{*\nu} - \bar{K}^{*\nu}\rho^\mu\left(\partial_\mu K^*_\nu - \partial_\nu K^*_\mu\right) - \bar{K}^{*\mu}\left(\partial_\mu \rho_\nu - \partial_\nu \rho_\mu\right)K^{*\nu}\right\} \tag{A11}$$

$$\mathcal{L}_{\omega K^* K^*} = i\frac{g}{2}\left\{\omega^\mu\left(\partial_\mu \bar{K}^*_\nu - \partial_\nu \bar{K}^*_\mu\right)K^{*\nu} - \omega^\mu \bar{K}^{*\mu}\left(\partial_\mu K^*_\nu - \partial_\nu K^*_\mu\right) - \left(\partial_\mu \omega_\nu - \partial_\nu \omega_\mu\right)\bar{K}^{*\mu}K^{*\nu}\right\} \tag{A12}$$

$$\mathcal{L}_{\phi K^* K^*} = -i\frac{g}{\sqrt{2}}\left\{\phi^\mu\left(\partial_\mu \bar{K}^*_\nu - \partial_\nu \bar{K}^*_\mu\right)K^{*\nu} - \phi^\mu \bar{K}^{*\mu}\left(\partial_\mu K^*_\nu - \partial_\nu K^*_\mu\right) - \left(\partial_\mu \phi_\nu - \partial_\nu \phi_\mu\right)\bar{K}^{*\mu}K^{*\nu}\right\} \tag{A13}$$

From Eq. (14):

$$\mathcal{L}_{\phi\rho K^* K^*} = \frac{g^2}{2\sqrt{2}}\phi^\mu\left(\bar{K}^*_\mu \rho^\nu K^*_\nu + \bar{K}^*_\nu \rho^\nu K^*_\mu - 2\bar{K}^*_\nu \rho_\mu K^{*\nu}\right) \tag{A14}$$

$$\mathcal{L}_{\phi\omega K^* K^*} = \frac{g^2}{2\sqrt{2}}\left\{\phi^\mu\omega^\nu\left(\bar{K}^*_\mu K^*_\nu + \bar{K}^*_\nu K^*_\mu\right) - 2\phi^\mu\omega_\mu \bar{K}^{*\nu}K^*_\nu\right\} \tag{A15}$$

$$\mathcal{L}_{\phi\phi K^* K^*} = -\frac{g^2}{2}\left(\phi^\mu\phi^\nu \bar{K}^*_\mu K^*_\nu - \phi^\mu\phi_\mu \bar{K}^{*\nu}K^*_\nu\right) \tag{A16}$$

From Eq. (21):

$$\mathcal{L}_{\phi K^* K\pi} = -\frac{ag^2}{4\sqrt{2}}\frac{c_V}{\sqrt{1+c_A}}\phi^\mu\left(\bar{K}^*_\mu \pi K + \bar{K}\pi K^*_\mu\right) \tag{A17}$$

$$\mathcal{L}_{\phi\phi KK} = -\frac{ag^2}{2}\frac{c_V}{1+c_A}\phi^\mu\phi_\mu \bar{K}K\,. \tag{A18}$$

APPENDIX B: K AND K^* DECAY WIDTHS

For the kaon:

$$\Gamma_{K\to\rho\,K}(s) = \frac{3a^2g^2}{32\pi}\frac{1}{(1+c_A)^2}\frac{p^3_{cm}(s,m_K,m_\rho)}{m^2_\rho}\,, \tag{B1}$$

$$\Gamma_{K\to\omega\,K}(s) = \frac{a^2g^2}{32\pi}\frac{1}{(1+c_A)^2}\frac{p^3_{cm}(s,m_K,m_\omega)}{m^2_\omega}\,, \tag{B2}$$

$$\Gamma_{K\to\phi\,K}(s) = \frac{a^2g^2}{16\pi}\frac{(1+2c_V)^2}{(1+c_A)^2}\frac{p^3_{cm}(s,m_K,m_\phi)}{m^2_\phi}\,, \tag{B3}$$

$$\Gamma_{K\to\rho\,K^*}(s) = \frac{3g^2_{VVP}}{16\pi}\frac{1}{1+c_A}p^3_{cm}(s,m_{K^*},m_\rho)\,, \tag{B4}$$

$$\Gamma_{K\to\omega\,K^*}(s) = \frac{g^2_{VVP}}{16\pi}\frac{1}{1+c_A}p^3_{cm}(s,m_{K^*},m_\omega)\,, \tag{B5}$$

$$\Gamma_{K\to\phi\,K^*}(s) = \frac{g^2_{VVP}}{8\pi}\frac{(1+2c_{WZ})^2}{1+c_A}p^3_{cm}(s,m_{K^*},m_\phi)\,. \tag{B6}$$

For the K^*:

$$\Gamma_{K^*\to\pi\,K}(s) = \frac{a^2g^2}{32\pi}\frac{(1+c_V)^2}{1+c_A}\frac{p^3_{cm}(s,m_K,m_\pi)}{s}\,, \tag{B7}$$

$$\Gamma_{K^*\to\rho\,K}(s) = \frac{g^2_{VVP}}{16\pi}\frac{1}{1+c_A}p^3_{cm}(s,m_K,m_\rho)\,, \tag{B8}$$

$$\Gamma_{K^*\to\omega\,K}(s) = \frac{g^2_{VVP}}{48\pi}\frac{1}{1+c_A}p^3_{cm}(s,m_K,m_\omega)\,, \tag{B9}$$

$$\Gamma_{K^*\to\phi\,K}(s) = \frac{g^2_{VVP}}{24\pi}\frac{(1+2c_{WZ})^2}{1+c_A}p^3_{cm}(s,m_K,m_\phi)\,, \tag{B10}$$

$$\Gamma_{K^*\to\pi\,K^*}(s) = \frac{g^2_{VVP}}{16\pi}(1+2c_{WZ})^2 p^3_{cm}(s,m_{K^*},m_\pi)\,, \tag{B11}$$

$$\Gamma_{K^*\to\rho\,K^*}(s) = \frac{g^2}{8\pi}\frac{p^2_{cm}(s,m_{K^*},m_\rho)+3m^2_{K^*}}{m^2_{K^*}\,m^2_\rho}\times p^3_{cm}(s,m_{K^*},m_\rho)\,, \tag{B12}$$

$$\Gamma_{K^*\to\omega\,K^*}(s) = \frac{g^2}{24\pi}\frac{p_{cm}^2(s,m_{K^*},m_\omega)+3m_{K^*}^2}{m_{K^*}^2\,m_\omega^2}\times$$
$$p_{cm}^3(s,m_{K^*},m_\omega)\,, \quad \text{(B13)}$$

$$\Gamma_{K^*\to\phi\,K^*}(s) = \frac{g^2}{12\pi}\frac{p_{cm}^2(s,m_{K^*},m_\phi)+3m_{K^*}^2}{m_{K^*}^2\,m_\phi^2}\times$$
$$p_{cm}^3(s,m_{K^*},m_\phi)\,. \quad \text{(B14)}$$

Here, s is the invariant mass squared of the K or K^*, which coincides with the CM energy squared for s-channel diagrams, and $p_{cm}(s,m_1,m_2)$ is the CM three-momentum of the outgoing particles.

APPENDIX C: BETHE-SALPETER EQUATION FOR THE VVVV AMPLITUDE

Let us consider the elastic reaction $\phi(p_1)+K^*(p_2)\to\phi(p_3)+K^*(p_4)$. The contact term amplitude, given by

$$\begin{aligned}\mathcal{M}_{full} &= \alpha g^2\{\epsilon_\mu(p_1)\epsilon_\nu(p_2)\epsilon_\mu(p_3)\epsilon_\nu(p_4)\\ &+ \epsilon_\mu(p_1)\epsilon_\mu(p_2)\epsilon_\nu(p_3)\epsilon_\nu(p_4)\\ &- 2\epsilon_\mu(p_1)\epsilon_\nu(p_2)\epsilon_\nu(p_3)\epsilon_\mu(p_4)\}\,, \quad \text{(C1)}\end{aligned}$$

where $\epsilon_\mu(p)$ is the polarization vector and $\alpha=-1/2$, is too involved so that solving the BS equation for it becomes impracticable. Instead, we take a part of the full amplitude

$$\mathcal{M}_{part} = \alpha g^2\epsilon_\mu(p_1)\epsilon_\mu(p_2)\epsilon_\nu(p_3)\epsilon_\nu(p_4) \quad \text{(C2)}$$

for which the equation becomes algebraic. It is easy to see that the solution looks like

$$\mathcal{M}_{part}^{BS} = f^2(s)\epsilon_\mu(p_1)\epsilon_\mu(p_2)\epsilon_\nu(p_3)\epsilon_\nu(p_4) \quad \text{(C3)}$$

with

$$f^2(s) = \frac{\alpha g^2}{1+\alpha g^2 G(s,m_\phi,m_{K^*})} \quad \text{(C4)}$$

and

$$\begin{aligned}G(s,m_\phi,m_{K^*}) &= -i\int\frac{d^4q}{(2\pi)^4}D_{K^*}^{\mu\nu}\left(\frac{p_1+p_2}{2}+q\right)\times\\ &D_{\phi\,\mu\nu}\left(\frac{p_1+p_2}{2}-q\right)\,. \quad \text{(C5)}\end{aligned}$$

Neglecting the real part of the propagators (K-matrix approximation)

$$\frac{1}{p^2-m^2+i\epsilon}\to-(2\pi i)\delta(p^2-m^2) \quad \text{(C6)}$$

one obtains Eq. (38) for G. Then, we extrapolate Eq. (C4) to the case of inelastic reactions assuming that it can be separated into to factors: one corresponding to the incoming pair of particles and another to the outgoing one, arriving this way at Eq. (37).

Even if $\mathcal{M}_{part}$ is not the correct tree-level amplitude, we believe that using Eq. (C4), or (37), instead of the factor αg^2 takes fairly well into account the corrections to $\mathcal{M}_{full}$ arising from the resummation of s-channel loops. We have actually studied the non-relativistic case, where the BS equation for $\mathcal{M}_{full}$ also becomes algebraic, finding that the ratios $\mathcal{M}_{full}^{BS}/\mathcal{M}_{full}^{BS}$ and $\mathcal{M}_{part}^{BS}/\mathcal{M}_{part}^{BS}$ are very similar, at least for moderate values of s.

[1] J. Rafelski and B. Muller, Phys. Rev. Lett. **48**, 1066 (1982).
[2] A. Shor, Phys. Rev. Lett. **54**, 1122 (1985).
[3] M. Asakawa and C. M. Ko, Nucl. Phys. **A572**, 732 (1994).
[4] C. Song, Phys. Lett. **B388**, 141 (1996), hep-ph/9603259.
[5] M. Asakawa and C. M. Ko, Phys. Lett. **B322**, 33 (1994), nucl-th/9401016.
[6] C. M. Ko and D. Seibert, Phys. Rev. **C49**, 2198 (1994), nucl-th/9312010.
[7] K. Haglin, Nucl. Phys. **A584**, 719 (1995), nucl-th/9410028.
[8] W. Smith and K. L. Haglin, Phys. Rev. **C57**, 1449 (1998), nucl-th/9710026.
[9] S. V. Afanasiev et al. (NA49), Phys. Lett. **B491**, 59 (2000).
[10] M. C. Abreu et al. (NA38), Phys. Lett. **B368**, 239 (1996).
[11] M. C. Abreu et al. (NA50), J. Phys. **G27**, 405 (2001).
[12] D. Rohrich, J. Phys. **G27**, 355 (2001).
[13] K. Safarik, J. Phys. **G27**, 579 (2001).
[14] S. C. Johnson, B. V. Jacak, and A. Drees, Eur. Phys. J. **C18**, 645 (2001), nucl-th/9909075.
[15] M. Bando, T. Kugo, and K. Yamawaki, Phys. Rept. **164**, 217 (1988).
[16] M. Bando, T. Kugo, and K. Yamawaki, Nucl. Phys. **B259**, 493 (1985).
[17] M. Bando, T. Kugo, S. Uehara, K. Yamawaki, and T. Yanagida, Phys. Rev. Lett. **54**, 1215 (1985).
[18] M. Benayoun et al., Eur. Phys. J. **C2**, 269 (1998), hep-ph/9707509.
[19] M. Benayoun and H. B. O'Connell, Phys. Rev. **D58**, 074006 (1998), hep-ph/9804391.
[20] A. Bramon, A. Grau, and G. Pancheri, Phys. Lett. **B345**, 263 (1995), hep-ph/9411269.

[21] T. Fujiwara, T. Kugo, H. Terao, S. Uehara, and K. Yamawaki, Prog. Theor. Phys. **73**, 926 (1985).
[22] A. Bramon, A. Grau, and G. Pancheri, Phys. Lett. **B344**, 240 (1995).
[23] C. Caso et al. (Particle Data Group), Eur. Phys. J. **C3**, 1 (1998).
[24] H. Leutwyler and M. Roos, Z. Phys. **C25**, 91 (1984).
[25] T. Biro, H. W. Barz, B. Lukacs, and J. Zimanyi, Phys. Rev. **C27**, 2695 (1983).
[26] C. M. Ko and L.-H. Xia, Phys. Rev. **C38**, 179 (1988).
[27] J. D. Bjorken, Phys. Rev. **D27**, 140 (1983).
[28] E. Schnedermann and U. Heinz, Phys. Rev. **C47**, 1738 (1993).
[29] J. Sollfrank et al., Phys. Rev. **C55**, 392 (1997), nucl-th/9607029.
[30] H. Bebie, P. Gerber, J. L. Goity, and H. Leutwyler, Nucl. Phys. **B378**, 95 (1992).
[31] C. Song and V. Koch, Phys. Rev. **C55**, 3026 (1997), nucl-th/9611034.
[32] R. Rapp and E. V. Shuryak, Phys. Rev. Lett. **86**, 2980 (2001), hep-ph/0008326.
[33] R. A. Schneider and W. Weise, Phys. Lett. **B515**, 89 (2001), hep-ph/0102189.